INSTRUMENTATION AND MEASUREMENT

A Yb optical clock with a lattice power enhancement cavity

Chunyun Wang(王春云), Yuan Yao(姚远)[†], Haosen Shi(师浩森), Hongfu Yu(于洪浮), Longsheng Ma(马龙生), and Yanyi Jiang(蒋燕义)[‡]

State Key Laboratory of Precision Spectroscopy, East China Normal University, Shanghai 200062, *China*

(Received 6 November 2023; revised manuscript received 19 December 2023; accepted manuscript online 29 December 2023)

We construct a power enhancement cavity to form an optical lattice in an ytterbium optical clock. It is demonstrated that the intra-cavity lattice power can be increased by about 45 times, and the trap depth can be as large as $1400E_r$ when laser light with a power of only 0.6 W incident to the lattice cavity. Such high trap depths are the key to accurate evaluation of the lattice-induced light shift with an uncertainty down to $\sim 1\times10^{-18}$. By probing the ytterbium atoms trapped in the power-enhanced optical lattice, we obtain a 4.3 Hz-linewidth Rabi spectrum, which is then used to feedback to the clock laser for the close loop operation of the optical lattice clock. We evaluate the density shift of the Yb optical lattice clock based on interleaving measurements, which is $-0.46(62)$ mHz. This result is smaller compared to the density shift of our first Yb optical clock without lattice power enhancement cavity mainly due to a larger lattice diameter of 344 μm.

Keywords: optical atomic clock, optical lattice, optical cavity, Stark shift

PACS: 06.20.fb, 42.79.Gn, 95.55.Sh, 37.10.Jk **DOI:** 10.1088/1674-1056/ad1986

1. Introduction

In the last decade, the development of optical atomic clocks has drawn wide attention since they can provide unprecedented measurement precision and uncertainty at the 10^{-18} level.[1–4] Nowadays, optical atomic clocks play a significant role in tests of fundamental physics,[5–7] search for dark matter,[8,9] and precision measurement.[10,11] Most importantly, the international system of units (SI) of time, the second, will be redefined based on the optical atomic clocks.[12,13] Optical clocks based on a large number of neutral atoms trapped in an optical lattice (also called optical lattice clocks) have shown advantages in frequency stability. Due to thousands of atoms contributing to the signal, optical lattice clocks have lower frequency instabilities on the $10^{-16}/\sqrt{\tau}$ level[8,14] and thus it takes less time to achieve a measurement uncertainty of 10^{-18} in frequency ratio measurements.[8]

However, in optical lattice clocks the lattice light usually has a large power in order to trap enough atoms, resulting in nonnegligible frequency shifts. The shifts of the ground and the excited electronic levels can be cancelled by carefully tuning the lattice laser frequency close to a magic wavelength,[15] which will largely reduce the resulting frequency shift of the clock transition. As the frequency uncertainty of optical lattice clocks has been pushed down below 10^{-17}, high order couplings, including magnetic dipole, electric quadrupole, and hyper-polarizability should be considered.[16–19] However, the uncertainties of the frequency shift coefficients due to multi-polarizability and hyperpolarizability are the key limitation when reducing the uncertainty of lattice light shift below 2×10^{-18}.[17,20,21] One approach to accurately determine these coefficients is to measure the frequency shifts when the trap depth varies from tens of recoil energy to even thousands of recoil energy,[16,17] which challenges the output power of lattice lasers. A power enhancement lattice cavity can solve this problem.[16,18,19] Meanwhile, the implement of a lattice power enhancement cavity has three other benefits. First, due to power enhancement the lattice intensity can be kept unchanged when the lattice beam waist is increased in order to reduce the collision shift and the collision loss of trapped atoms as well. The exclusion of the frequency shifts due to atomic collision is a prerequisite in determining the higher-order lattice shift coefficients.[16,17] Second, the lattice light in the cavity is a standing wave, and the intensities of two propagating lattice beams are balanced. Thus, the frequency shift due to imbalanced lattice intensity can be ignored.[1,17] Third, due to power enhancement, it reduces the light power of the lattice laser, and thus the power consumption and size. This additional benefit is critical in transportable optical clocks for practical applications such as geopotential measurement.[22,23]

In this paper, we design and construct a power enhancement cavity to form an optical lattice for ytterbium (Yb) atoms. The waist diameter of the intra-cavity lattice light is 344 μm, large enough to significantly reduce the atomic density and thereby the frequency shift due to atomic collision. Experimentally, we succeed in loading thousands of ^{171}Yb atoms from the magneto-optical trap (MOT) into the cavity-enhanced optical lattice with a trap depth U set in the range of $13E_r$–$1400E_r$, where E_r is the lattice photon recoil energy. The intra-

[†]Corresponding author. E-mail: yyao@lps.ecnu.edu.cn
[‡]Corresponding author. E-mail: yyjiang@phy.ecnu.edu.cn

cavity lattice power is increased by about 45 times. Such trap depths support accurate evaluation of the frequency shift of optical atomic clocks due to the lattice light. Moreover, based on interleaving measurements we evaluate the density shift of the Yb optical lattice clock to be $-0.46(62)$ mHz, smaller compared to that of our first Yb optical lattice clock mainly due to a larger lattice waist.

2. Experimental setup

The schematic diagram of the optical clock based on Yb atoms trapped in a cavity-enhanced optical lattice is shown in Fig. 1. Laser cooling and trapping Yb atoms are similar to our previous work.[24,25] In brief, ^{171}Yb atoms flying from an effusive oven are slowed down by absorbing an opposite propagation laser light at 399 nm, whose frequency is red-detuned from the $^1S_0$–$^1P_1$ transition. The upper inset in Fig. 1 shows the related energy levels of Yb atoms. Then the slowed atoms are trapped and cooled in a two-stage MOT, the first stage on the $^1S_0$–$^1P_1$ transition and the second on the $^1S_0$–$^3P_1$ transition. Consequently, nearly 10^5 atoms with a temperature of about 15 μK are ready for loading into an optical lattice.

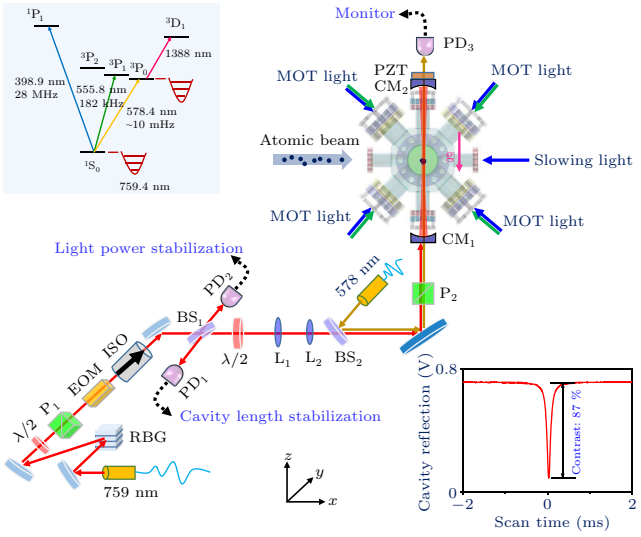

Fig. 1. Schematic of the vertically-oriented lattice build-up cavity using out-of-vacuum cavity mirrors CM_1 and CM_2. The inset figures show the cavity reflection (DC output voltage of PD_1) and the relevant energy levels of Yb atoms.

The lattice laser light at 759 nm is from a Ti: sapphire continuous wave (c.w.) laser via a piece of polarization maintenance (PM) optical fiber. At the output of the PM fiber, it is reflected on a reflective Bragg grating (RBG) with a spectral bandwidth of 0.05 nm to reduce background spectra-induced Stark shift.[26] The diffraction efficiency of the RBG is $\sim 90\%$ depending on the spatial mode of the input light. Then the diffracted light is phase-modulated at ~ 50 MHz in an electro-optic modulator (EOM). The polarization of the light incident onto the EOM is aligned along the principal axis of the EO crystal to reduce undesired amplitude modulation, and an optical isolator (ISO) is placed after the EOM to prevent the cavity reflection light back into the EOM. A portion of the light after ISO is detected on a DC photo detector (PD_2) to realize light power stabilization via adjusting the driving power of an acousto-optic modulator before the PM fiber (not shown in the figure). The transmitted laser light of the beam splitter (BS_2) combines with laser light at 578 nm (clock laser on the transition of $^1S_0$–$^3P_0$). Two lenses are placed before BS_2 for mode matching of the 759 nm laser light with the lattice cavity. The polarizations of the 578 nm laser light and the lattice laser light are purified and matched on a polarizer (P_2) before coupling into the lattice cavity. As shown in Fig. 1, all the optics before P_2 are horizontally located on a platform.

In our previous system, 759 nm laser light with a power of 230 mW is focused, and it is retro-reflected by a curved mirror to build up an optical lattice, which has a trap depth of $80E_r$ and a radius of 55 μm. The intensity of the retro-reflected beam of the lattice is attenuated to 85% of the incident lattice light. In this work, a power enhancement lattice cavity is composed of two high-reflective mirrors, CM_1 and CM_2, with a curvature of 250 mm separated by ~ 20 cm. With the same number of atoms, a waist radius of 172 μm in the transverse plane enables a relatively low atomic density and thus a small density-dependent collisional shift. The cavity is formed vertically in order to lift degeneracy among different lattice sites and to suppress tunneling.[27] The curved mirrors of CM_1 and CM_2 are placed outside of the vacuum chamber. By measuring the cavity linewidth $\Delta\nu_{cav}$ (3.77 MHz), cavity reflection R_{cav} (as shown in the inset of Fig. 1), cavity transmission T_{cav} of both an empty cavity and a cavity with vacuum windows placed inside the cavity, the transmissions of CM_1 and CM_2 are measured to be $T_{in} \sim 1\%$ and $T_{out} \sim 0.015\%$ at 759 nm, respectively. The loss L_w of each vacuum chamber window is $\sim 0.5\%$ at 759 nm. Thereby, the power-enhancement factor of the lattice cavity is estimated to be ~ 41 according to[28]

$$G = 4 \times T_{in} \times \left(\frac{F}{2\pi}\right)^2, \tag{1}$$

where $F = 2\pi/L_{tot}$ is the finesse of the lattice cavity, and $L_{tot} = T_{in} + T_{out} + 4L_w$ is the total loss of the cavity. In this work, $F \sim 199$.

The cavity reflected laser light at 759 nm is steered onto PD_1. By demodulating the AC signal from PD_1 with the driving signal of the EOM on a double balanced mixer, we obtain an error signal (the Pound–Drever–Hall signal[29]) related to the cavity resonance detuning from the 759 nm laser frequency. Such an error signal is then used to tune the voltage applied to a piezo (PZT) attached to the output mirror of the lattice cavity, CM_2. As long as the cavity is locked to the 759 nm laser light, the laser light can be resonant inside the

cavity, and the cavity transmission light can be detected on PD_3. In order to largely reduce the frequency shift due to the lattice light, the frequency of the 759 nm laser can be stabilized close to the magic wavelength via an optical frequency comb.[30]

3. Method and results

We load the atoms into the vertically-oriented one-dimensional optical lattice. In order to obtain enough atoms trapped in the optical lattice, we set the initial trap depth U_i in the range of $180E_r$–$270E_r$. The lattice photon recoil energy is

$$E_r = \frac{(h\nu_{lat})^2}{2m_{Yb}c^2} = h \times 2.02\ \text{kHz}, \tag{2}$$

where h is the Planck constant, c is the speed of light, ν_{lat} is the lattice laser frequency, and m_{Yb} is the mass of the ^{171}Yb atom. By the end of the green MOT, we keep the lattice depth at U_i for another 20 ms, and then we ramp the lattice depth to a desired value in 50 ms, as shown in Fig. 2(a). By ramping the lattice power, we can load more atoms into the lattice, i.e., nearly three times as that without ramping the lattice power.

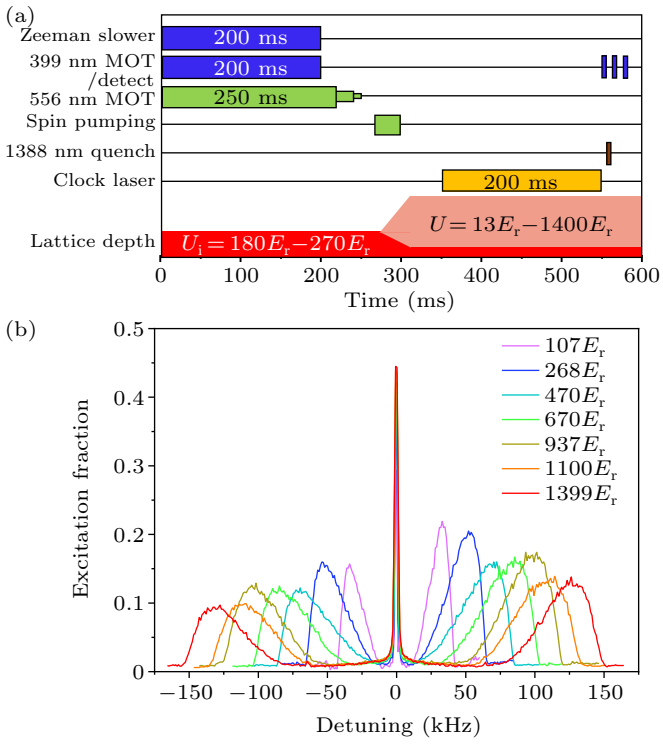

Fig. 2. (a) Experimental timing sequence of the Yb optical clock. (b) Motional sideband spectra at different trap depths, shown as the excitation fraction of the $^3P_0$ state versus laser frequency detuned from the $^1S_0$–$^3P_0$ clock transition.

After the Yb atoms are trapped in the lattice, we shine the clock laser light at 578 nm on the lattice-trapped atoms to excite the $^1S_0$–$^3P_0$ transition. The transmissions of CM_1 and CM_2 are $> 99\%$ at 578 nm. The population in the $^3P_0$ states is then measured in sequence using electron shelving detection.[31] Figure 2(b) shows the motional sideband spectra at different lattice depths. From the figure, we can deduce the trap depth U, longitudinal atomic temperature and vibrational state.[32] The longitudinal atomic temperature ranges from 1 μK to 25 μK when U is set in the range of $13E_r$–$1400E_r$. When the power of the 759 nm laser light incident onto the cavity is ~ 600 mW, the trap depth approaches to $1400E_r$, the highest to date. Such a wide tuning range of the trap depth is suitable for experimental evaluation of the lattice-induced light shifts.[15,16] From the trap depth U, we can deduce the lattice power sensed by the atoms. Thereby the power-enhancement factor is measured to be $G \sim 45$. For normal operation of a Yb atomic clock, the trap depth can be set to $\leq 50E_r$ in order to reduce the lattice light shift. Here we can trap ~ 1000 ^{171}Yb atoms when the trap depth U is lowered to $13E_r$. In that case, the power of the incident lattice light before the cavity is only ~ 10 mW.

With enough ^{171}Yb atoms trapped in the power enhancement lattice cavity, we then probe the clock transition of Yb atoms with Rabi spectroscopy by stepping the 578 nm laser frequency. The atoms are prepared to either one of the two nuclear spin states of $^1S_0$ by depleting the other spin state using a pumping light at 556 nm at a certain frequency and then decaying to the ground state. Three pairs of Helmholtz coils are employed to cancel the static stray magnetic field in three directions and to provide a bias magnetic field $\boldsymbol{B}$ to split the nuclear spin state degeneracy. The magnetic field $\boldsymbol{B}$ is oriented along with the polarization of the lattice light. When the atomic probe time is 200 ms and a single cycle time of 600 ms, a normalized excitation spectrum of the $^1S_0$ ($m_F = +1/2$)–$^3P_0$ ($m_F = +1/2$) clock transition with a spectral linewidth of ~ 4.3 Hz (full width at half-maximum, FWHM) and an excitation rate of ~ 0.8 at peak are observed, as shown in Fig. 3(a), comparable to that without power enhancement lattice cavity.[25] The spectrum in Fig. 3(a) is based on the ^{171}Yb atoms trapped in a lattice at a depth of $50E_r$. We also probe the clock transition of Yb atoms trapped in a lattice with a depth as low as $13E_r$, and similar Rabi spectra are observed.

Based on the above Rabi spectra, we use the measured excitation rate as a frequency discriminator to stabilize the frequency of the 578 nm laser to the atomic transition. To anticipate the frequency instability of the optical clock in a closed loop, we made an interleaved measurement,[25,33] which is close to a white noise model of $1.5 \times 10^{-15}/\sqrt{\tau}$, where τ is the averaging time.

By interleaving measurements at different atomic densities, the density shift is evaluated.[20,34] Assuming the same volume, the atomic density is proportional to the number of atoms. Here the number of atoms is set by changing the duration of the slower light at 399 nm during the first-stage

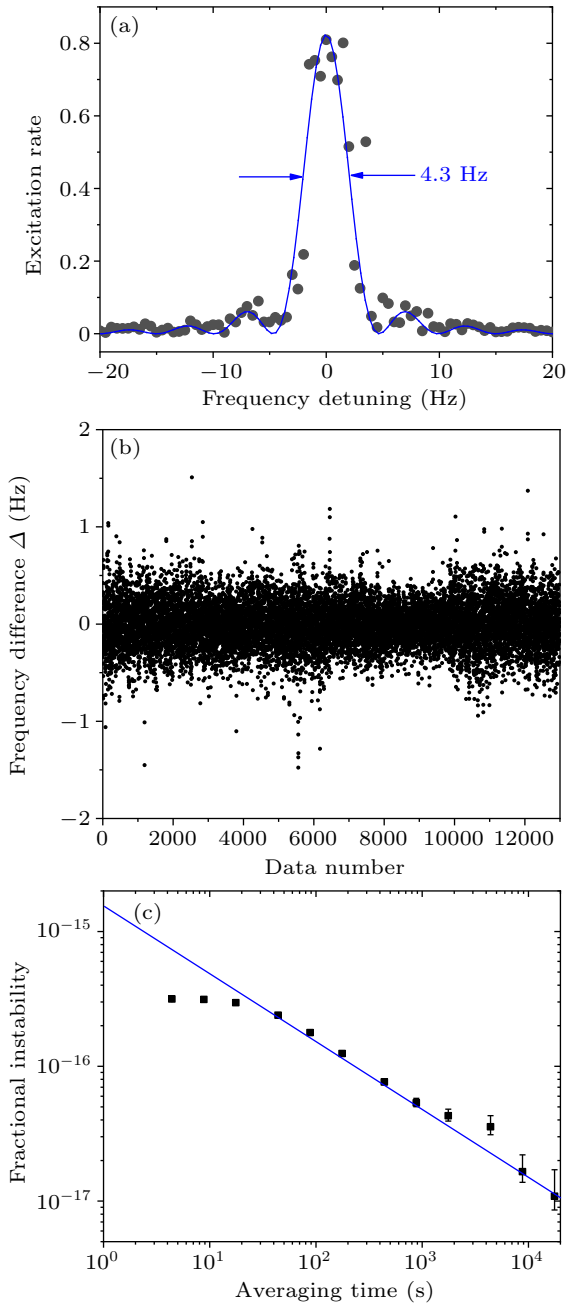

Fig. 3. (a) Rabi spectrum of the $^1S_0$ ($m_F = +1/2$)–$^3P_0$ ($m_F = +1/2$) clock transition of ytterbium atoms trapped in a cavity-enhanced optical lattice at a depth of $50E_r$. (b) Measured frequency difference Δ when the number of atoms is switched between $10N_{atom}$ and N_{atom}. (c) Fractional frequency instability of the interleaved measurement at two atomic densities. One-sigma error bars are shown.

MOT. Using this method, it does not impact the trapping conditions, and thus the density shift is proportional to the number of atoms.[21,35] When Yb atoms with an atomic temperature of 4 μK are trapped in the optical lattice at a trap depth of $U \sim 50E_r$, we measure the frequency difference of Δ when the number of atoms is switched between $10N_{atom}$ and N_{atom} in each cycle, as shown in Fig. 3(b), where $N_{atom} \sim 10^3$ is the number of atoms in normal operation. A single cycle time is 550 ms. This frequency difference of Δ is measured to be $-4.1(5.6)$ mHz with the uncertainty determined by the standard deviation of the mean values of three sub-datasets (each sub-dataset is based on 4000 data points from Fig. 3(b)). Figure 3(c) shows the instability of the frequency difference between two atomic densities, which can reach 1.5×10^{-17} in an averaging time of 10^4 s. Assuming the frequency shift is proportional to the atomic density,[20,35] in normal operation at $N_{atom} \sim 10^3$, the typical density shift is estimated to be $\Delta \cdot N_{atom}/(10N_{atom} - N_{atom}) = -0.46(62)$ mHz.

The measured density frequency shift in the cavity enhanced optical lattice is smaller than our previous result of $-2.7(1.7)$ mHz, which is measured when the atoms are trapped in a normal lattice with a depth of $U \sim 80E_r$, a lattice waist diameter of 110 μm and an atomic temperature of 0.8 μK. In both cases, the excitation rate of Yb atoms is $\sim 50\%$. Since the collision shift is insensitive to the trap depth U when $U < 100E_r$,[17] the smaller density shift measured in this paper is majorly due to a larger lattice waist in spite of a higher atomic temperature.

4. Conclusion

We report a lattice power-enhanced ^{171}Yb optical clock. The intra-cavity lattice power can be enhanced by about 45 times. In our current setup, we can set the trap depth of the lattice in the range of $13E_r$–$1400E_r$, enabling us to accurately measure the frequency shift coefficients of the Yb optical clock due to lattice light in the next step. Meanwhile, it is possible to operate the Yb optical lattice clock in a low trap depth at $13E_r$ for a lower lattice light shift and a lower density shift, which will largely reduce the corresponding uncertainties down to $\sim 1 \times 10^{-18}$. In addition, the clock system can be more compact with less power consumption and a smaller size of the lattice laser.

Acknowledgments

Project supported by the National Natural Science Foundation of China (Grant Nos. 12334020 and 11927810) and the National Key Research and Development Program of China (Grant No. 2022YFB3904001).

References

[1] McGrew W F, Zhang X, Fasano R J, Schäffer S A, Beloy K, Nicolodi D, Brown R C, Hinkley N, Milani G, Schioppo M, Yoon T H and Ludlow A D 2018 *Nature* **564** 87
[2] Brewer S M, Chen J S, Hankin A M, Clements E R, Chou C W, Wineland D J, Hume D B and Leibrandt D R 2019 *Phys. Rev. Lett.* **123** 033201
[3] Oelker E, Hutson R B, Kennedy C J, Sonderhouse L, Bothwell T, Goban A, Kedar D, Sanner C, Robinson J M, Marti G E, Matei D G, Legero T, Giunta M, Holzwarth R, Riehle F, Sterr U and Ye J 2019 *Nat. Photonics* **13** 714
[4] Huntemann N, Sanner C, Lipphardt B, Tamm C and Peik E 2016 *Phys. Rev. Lett.* **116** 063001
[5] Takamoto M, Ushijima I, Ohmae N, Yahagi T, Kokado K, Shinkai H and Katori H 2020 *Nat. Photonics* **14** 411
[6] Sanner C, Huntemann N, Lange R, Tamm C, Peik E, Safronova M S and Porsev S G 2019 *Nature* **567** 204

[7] Chou C W, Hume D B, Rosenband T and Wineland D J 2010 *Science* **329** 1630

[8] Beloy K, Bodine M I, Bothwell T, *et al.* 2021 *Nature* **591** 564

[9] Wcisło P, Ablewski P, Beloy K, Bilicki S, Bober M, Brown R, Fasano R, Ciuryło R, Hachisu H, Ido T, Lodewyck J, Ludlow A, McGrew W, Morzyński P, Nicolodi D, Schioppo M, Sekido M, Le Targat R, Wolf P, Zhang X, Zjawin B and Zawada M 2018 *Sci. Adv.* **4** eaau4869

[10] Bothwell T, Kennedy C J, Aeppli A, Kedar D, Robinson J M, Oelker E, Staron A and Ye J 2022 *Nature* **602** 420

[11] Kolkowitz S, Pikovski I, Langellier N, Lukin M D, Walsworth R L and Ye J 2017 *Phys. Rev. D* **94** 124043

[12] https://www.bipm.org/documents/20126/35554894/CCTF+Strategy/7cf0f648-2afe-d15c-0909-1f03406bbb8f

[13] CCTF 2021 *Roadmap towards the redefinition of the SI second*

[14] Ai D, Qiao H, Zhang S, Luo L M, Sun C Y, Zhang S, Peng C Q, Qi Q C, Jin T Y, Zhou M and Xu X Y 2020 *Chin. Phys. B* **29** 090601

[15] Katori H, Takamoto M, Pal'chikov V G and Ovsiannikov V D 2003 *Phys. Rev. Lett.* **91** 173005

[16] Brown R C, Phillips N B, Beloy K, McGrew W F, Schioppo M, Fasano R J, Milani G, Zhang X, Hinkley N, Leopardi H, Yoon T H, Nicolodi D, Fortier T M and Ludlow A D 2017 *Phys. Rev. Lett.* **119** 253001

[17] Nemitz N, Jørgensen A A, Yanagimoto R, Bregolin F and Katori H 2019 *Phys. Rev. A* **99** 033424

[18] Ushijima I, Takamoto M and Katori H 2018 *Phys. Rev. Lett.* **121** 263202

[19] Kim K, Aeppli A, Bothwell T and Ye J 2023 *Phys. Rev. Lett.* **130** 113203

[20] Kim H, Heo M S, Park C Y, Yu D H and Lee W K 2021 *Metrologia* **58** 055007

[21] Pizzocaro M, Bregolin F, Barbieri P, Rauf B, Levi F and Calonico D 2020 *Metrologia* **57** 035007

[22] Koller S B, Grotti J, Vogt S T, Al-Masoudi A, Dörscher S, Häfner S, Sterr U and Lisdat C H 2017 *Phys. Rev. Lett.* **118** 073601

[23] Zeng M, Huang Y, Zhang B, Hao Y, Ma Z, Hu R, Zhang H, Chen Z, Wang M, Guan H and Gao K 2023 *Phys. Rev. Appl.* **19** 064004

[24] Yan W, Yao Y, Sun Y, Chad H W, Jiang Y and Ma L 2019 *Chin. Opt. Lett.* **17** 040201

[25] Sun Y, Yao Y, Hao Y, Yu H, Jiang Y and Ma L 2020 *Chin. Opt. Lett.* **18** 070201

[26] Fasano R J, Chen Y J, McGrew W F, Brand W J, Fox R and Ludlow A D 2021 *Phys. Rev. Appl.* **15** 044016

[27] Lemonde P and Wolf P 2005 *Phys. Rev. A* **72** 033409

[28] Ye J 1997 *Ultrasensitive high resolution laser spectroscopy and its application to optical frequency standards* (PhD thesis)

[29] Drever R W P, Hall J L, Kowalski F V, Hough J, Ford G M, Munley A J and Ward H 1983 *Appl. Phys. B* **31** 97

[30] Hao Y, Yao Y, Shi H, Yu H, Jiang Y and Ma L 2022 *Chin. Opt. Lett.* **20** 120201

[31] Itano W M, Bergquist J C, Bollinger J J, Gilligan J M, Heinzen D J, Moore F L, Raizen M G and Wineland D J 2002 *Phys. Rev. A* **47** 3554

[32] Blatt S, Thomsen J W, Campbell G K, Ludlow A D, Swallows M D, Martin M J, Boyd M M and Ye J 2009 *Phys. Rev. A* **80** 052703

[33] Jiang Y Y, Ludlow A D, Lemke N D, Fox R W, Sherman J A, Ma L S and Oates C W 2011 *Nat. Photonics* **5** 158

[34] Lu B, Su Z, Yang T, Lin Y, Wang Q, Li Y, Meng F, Lin B, Li T and Fang Z 2022 *Chin. Phys. Lett.* **39** 080601

[35] Pizzocaro M, Thoumany P, Rauf B, Bregolin F, Milani G, Clivati C, Costanzo G A, Levi F and Calonico D 2017 *Metrologia* **54** 102